Redistribution of the residual welding stresses

Segen F. Estefen[1], Tetyana Gurova [1,2] and Anatoli Leontiev[3]

1 Subsea Technology Laboratory, COPPE, Federal University of Rio de Janeiro, Rio de Janeiro, Brazil

2 Shipbuilding Program, UEZO – Western State University, Rio de Janeiro, Brazil
  Correspondence author – E-mail: gurova@lts.coppe.ufrj.br

3 Institute of Mathematics, Federal University of Rio de Janeiro, Rio de Janeiro, Brazil

Abstract

This paper presents an experimental study of the residual welding stresses for butt-jointed steel plates. The stresses were monitored over two weeks after the removal of the welding constraints. The measurements were performed at the deposited metal, the heat--affected zone, the base metal close to the weld joint and along the plate using the X-ray diffraction method. The experimental results showed the continuous process of welding stress relaxation over a relatively short length of time. The observed stress redistribution trend was characterized by a reduction in and a uniformity of the values of the maximum shear stresses.

1   Introduction

Residual stresses due to welding can significantly affect the engineering properties of materials and structural components. Metallurgical processes during welding, such as shrinkage, quenching, and phase transformations, produce both tensile and compressive residual stresses in different zones of the welded parts, Macherauch, E., and Wohlfahrt, H., (1997). These residual stresses, particularly tensile stresses, can significantly impact the reliability and the integrity of the welded components. Systematic studies have shown that residual stresses may result in failure mechanisms that are sensitive to localized stresses, such as the following: fatigue, brittle fracture, stress corrosion cracking, and creep cracking. Therefore, it is important to understand the distribution of the residual stresses on the surface of the welded components in and near the welding zone. New techniques for measurements, improvements in equipment, and advances in computational methods have stimulated both numerical and experimental studies of welding processes, see Gannon, L. et al (2010), Paradowska, A,M. et al (2009) and Deng, D. and Murakawa, H., (2008).

The residual stress distributions developed in welded joints and structures are difficult to predict because of the complex dependence of the residual stress field upon many different factors, such as preexisting residual stresses in the parts being joined before welding, the material properties of the weld and the jointed parts, the geometry of the parts, the applied restraints, the welding procedure, including the weld preparation, the welding conditions and the pass sequence in multi-pass welding, the residual stresses generated or relaxed by manufacturing operations after the welding or by thermal and mechanical loading during the service life. The latest studies show, for example, that the final residual welding stresses depend strongly on the clamping conditions as well, especially

the clamping time, the release time and the clamp preheating, Schenk, T. et al (2009).

In this paper, the behavior of the welding stresses was studied from the moment when the welding clamps were removed, and two different types of welding were analyzed, one with a single electrode and another with double electrodes. Double-electrode welding increases productivity because of faster deposit rates as compared with single-electrode welding. Many of the different characteristics of double-electrode welding have already been investigated, such as the process stability, the effects of the total current, the melting rate, the microstructure, and the heat affected zone (HAZ) hardness, see Li, K. and Zhang, Y.M., (2007), Li, K.H. and Zhang, Y.M., (2008) and Li, K.H. et al (2008). Single-electrode and double-electrode welding stress distributions are expected to be different because of their respective thermal regimes, quantity of melted material and, consequently, the effects of the phase transformations that occur in the deposited metal, the HAZ, and the base metal close to the weld fillet, Li, K.H. and Zhang, Y.M., (2008).
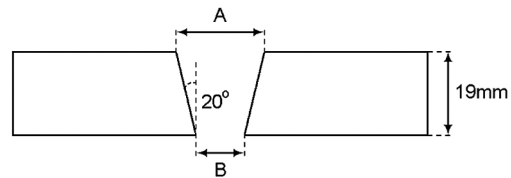
It is noted that the authors of measurement experiments almost never specify exactly how long after the removal of the clamps the welding stress measurements were performed. However, the numerical results of welding stress simulations correspond to the moment just after the cool down or the removal of the clamps. Thus, the authors that compare numerical and experimental welding stress results probably suppose that the welding stress distributions will not change with time upon completion of the welding procedure. Our experiments show over a relatively short length of time, two weeks after the removal of the clamps, the welding stress distribution undergoes a notable transformation, and the stresses only stabilize at the end of this process. This stress relaxation process is probably one of the reasons explaining the differences reported by some authors between the results of experimental welding stress measurements and the welding stresses estimated by computer simulations, see Aloraier, A. et al (2010).

2   Experimental arrangement

The experiments were performed using ASTM A131 grade A ferrite steel plates typically employed in the shipbuilding industry. The nominal yield strength of the plate material was 235 MPa, and the chemical composition is presented in Table 1. For each test, two plates were jointed with dimensions 1200 mm x 500 mm x 19 mm and a chamber angle of 20o (see Fig. 1). Specially designed tables were manufactured in order to support the plates and to provide the clamped conditions during the welding. The plates were restricted from out-of-plane displacements along the outside edges as shown in Fig. 2. The welding constraints were removed one day after welding.

Table 1   Chemical composition of material of the plate.

Element	Quantity (%)
Carbon	0.23
Iron	97.0
Manganese	2.73
Phosphorus	0.035
Sulfur	0.040

Fig. 1   Chamber details. Single-electrode welding: A=20mm, B=6mm; Double-electrode welding: A=18mm, B=4mm.

Fig. 2   Plates fixed by clamps along the edges on the support table and automatic double-electrode welding machine.

Natural frequency of pipeline vibration in still water is used to calculate the Reduced Velocity (V_R=U/f_n x D_o). And, the added mass coefficient (C_a) is determined from the linear interpolation in V_R, from the experimental data presented by Vikestad (1998) for elastic mounted rigid cylinder, as in Fig. 2, in Re number ranging from 14,000 to 65,500. The cylinder is restrained to move only in the cross-flow direction, and end-plates are fit at the both cylinder ends. The mass ratio is 1.306 (without the added mass) and the damping ratio is around 0.1% (in air). The maximum vibration amplitude is A_{CF}/ D_o ≈ 1.15 and it is found for V_R ≈ 6.0. Vikestad (1998) observed a good agreement of added mass coefficients for an oscillating rigid cylinder obtained from experiment, when compared with the other ones (Sarpkaya, 1978; Gopalkrishnan, 1993). Finally, with the C_a, the 'true' natural frequency is calculated by performing the Eigenvalue analysis with the added-mass matrix [M_a] updated.

The welding procedure was performed automatically by a welding machine with tandem arc as shown in Fig. 2. Welding data are presented in Table 2. For both cases, the employed electrode was a 1.2 mm carbon steel rod, Supercored 70NS, identified by the specification AWS A5.18/ASME SFA5.18 E70C-6M with a yield strength of 440 MPa.
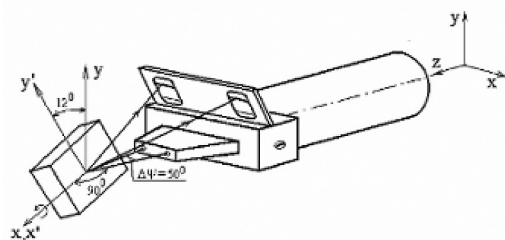
Table 2   Double-electrode welding data.

Pass	Electrode	U(V)	I(A)	Welding Speed (cm/min)
1	1	28.0	325.0	30.0
1	2	25.2	244.0	30.0
2	1	30.6	373.0	30.0
2	2	28.6	280.0	30.0
3	1	33.6	361.0	30.0
3	2	32.6	270.0	30.0

3   Stress measurement methodology

The absolute values of the stresses were measured on the top side of the plate surface by the X-ray diffraction method using the portable equipment RAYSTRESS, which employs the method of double exposure, Monin, V. et al (2000). This measuring technique has been widely tested and successfully employed in many different practical engineering applications, see Gurova, T. et al (1997-a), Gurova, T. et al (1997-b), Gurova, T. et al (1998), Monin, V. et al (2000), Monin, V. et al (2001-a), Monin, V. et al (2001-b) and Assis, J.T. et al (2002).

The principle of the stress measurements is demonstrated in Fig. 3. Two cassette windows capture the diffraction lines in 2θ angular intervals from 148° to 164°. Inclination of the specimen surface of 12o corresponds to measurements for steel specimens using Cr-K$_\alpha$ radiation and {211} reflection with θ_{211}=78º.

When using the X-ray diffraction method to measure weld stresses, some authors pay special attention to the stress-free lattice spacing. The hypothesis that the change of this lattice spacing across the weld due to microstructural variations affects the results of the stress measurements has been explored, for example, in the paper Korsunsky, A.M. et al (2007).

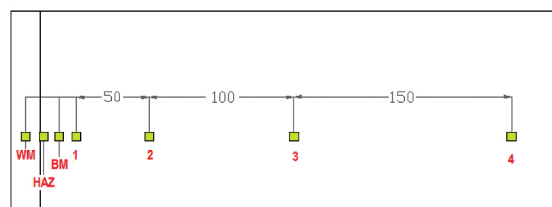Fig. 3   Location of the residual stress measuring points.

To adjust the experimental stress measurement results, a least squares optimization problem is solved by considering the unstrained lattice spacing as a control parameter. The optimal solution guarantees that the measured stress is close to the theoretically predicted value at a certain set of measurement points. Then, the obtained optimal lattice spacing is used to recalculate the stress at the rest of the measurement points. However, experimental results by Paradowska, A. et al (2006) have shown that there is no significant variation of the stress-free lattice spacing, and thus, we assume here that the interplanar distance d0 does not change across the weld.

Figures 4a and 4b present C_L and φ against A_{CF} / D_o and StU/fD, respectively. Results for oscillating horizontal rigid cylinder experiments in Staubli (1983) show similar trends for C_L and φ, respectively. From Fig. 4a, C_L increases with A_{CF}/D_o and the maximum values happen for StU/fD < 1. Thus, as larger is the C_L bigger is the amplitude of vibration, for f larger than the natural frequency of vortex shedding. It agrees with the high values of C_{dv} found at this region (Fig. 3a). In Fig. 4b, signal inversion can be observed for φ. It is a consequence of the quick decrease of C_{mv} when f approaches to the natural frequency of vortex shedding (Fig. 3b). Experiments in Williamson and Rosko (1983) have shown that in lock-in condition, this jump for φ happens, and it could be related to the change of the vortex shedding pattern.

4   Experimental results

The X-ray residual stress measurements for each pair of joined plates were performed along the mid-plate perpendicular to the weld line at four different points (1–4) spaced 50, 100, and 150 mm from each other as well as at the points along the deposited metal (WM), the heat-affected zone (HAZ) and the base metal close to the weld fillet (BM). The BM point was spaced 10 mm from the HAZ point, and point (1) was spaced 10 mm from the BM point, see Fig. 4.

Fig. 4   Scheme of stress measurements with RAYSTRESS equipment.

At each point, the stresses were measured in two directions, parallel to the weld (longitudinal stress) and perpendicular to the weld (transverse stress). Additional measurements at each measuring point directed at a 45 degree angle with respect to the used measuring directions show that the stresses measured in the longitudinal and the transverse directions were the principal stress directions near the weld fillet and are close to the principal stress directions at the other measuring points. This result is expected from a theoretical point of view due to symmetry, and

it allows us to obtain the maximum shear stress values as a half of the modulus of the difference between the measured stresses in the longitudinal and the transverse directions.

Electro-chemical etching to a depth of 0.2 mm was applied both to guarantee the absence of mechanical stress induced on the plate surface by manufacturing or collateral procedures and to identify the limits of the HAZ. Registration of {211} diffraction lines with the Cr-Ka wavelength were used for the X-ray analysis. The magnitudes of the X-ray elastic constants were taken from Hauk, V., (1997). The beam spot dimensions were 0.5 mm x 6 mm. The experimental accuracy of the stress measurements was 20 MPa. Measurements of the stresses in arbitrary directions in the plates before welding showed the presence of residual tensile stresses between 20 and 40 MPa caused by the thermo-mechanical treatments of the plates during fabrication.

The stress measurements were performed two days after welding and two weeks after welding. During the two weeks period the welded plates remained on the support table at the laboratory conditions and ambient temperature from 26 to 30 degree Celsius. The two week period was chosen experimentally based on the results of the measured stresses. It was noted that after this period, the values of the measured stresses did not change. However, it is not possible to confirm that this is the minimum necessary time for the relaxation of the residual stresses. Even so, significant changes in the results of the measured stress distributions after two days and two weeks were observed for all the processes.
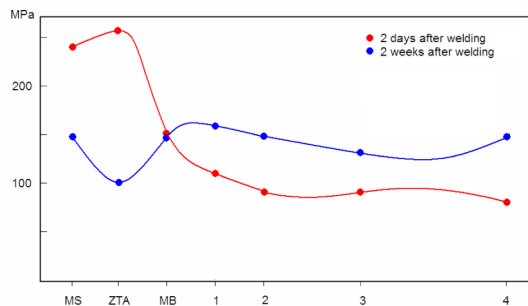

Fig. 5 Absolute values of the von Mises stresses for single-electrode welding.

A fuller picture of the welding stress redistribution emerged as the von Mises stress was observed, see Fig. 5 and Fig. 6.
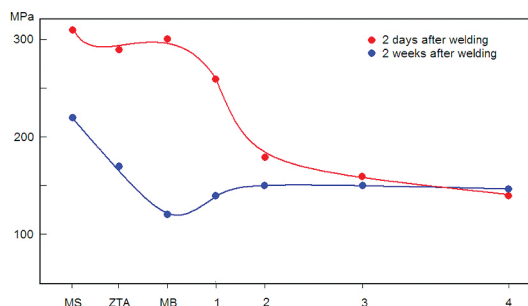

Fig. 6 Absolute values of the von Mises stresses for double-electrode welding.
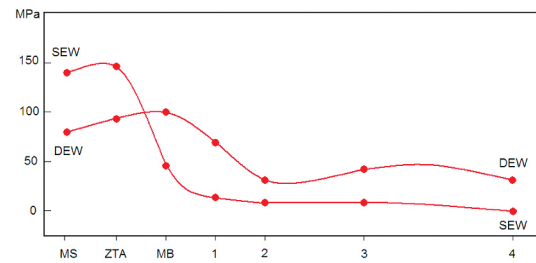

Fig. 7 Absolute values of maximum shear stresses for single-electrode (SEW) and double-electrode (DEW) welding in 2 days.
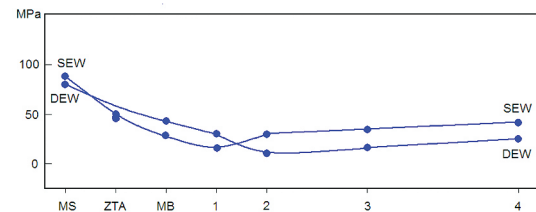

Fig. 8 Absolute values of maximum shear stresses for single-electrode (SEW) and double-electrode (DEW) welding in 2 weeks.

A 10 x 60 x 19 mm cross section of the weldments composed of the parent plate and the weld metal was removed transverse to the welding direction to produce specimens for examination of the microstructure. The weld metal microstructure was revealed using 2% Nital. The microstructure was evaluated using a standard optical microscope. The microstructure analysis demonstrated the absence of microcracks in the deposited metal, the heat affected zone and the base metal close to the weld joint on the welded specimens. Thus, the possibility that the observed welding stress relaxation was the result of material failure can be ruled out.

5   Conclusions

1. The experimental results obtained with two different techniques showed that the welding stress distribution for the butt-jointed steel plates underwent notable transformation over a period of two weeks after the completion of the welding procedure both for the single–electrode and the double–electrode welding techniques.

2. The final (two-week) welding stress state was characterized by a more uniform distribution of the maximum shear stresses with smaller absolute values than that for the constrained and initial (two-day) welding stress distribution.

3. The microstructure analysis of the welded specimens ruled out the possibility that the observed welding stress relaxation might be the result of material failure.

4. It seems to be reasonable for the welding stress measuring results to specify the moment of measuring upon completion of the welding procedure.

5. In order to compare the results of welding stress from numerical simulations with experimental data, the detailed numerical models of the welding process must include an analysis of the welding stress relaxation after the end of the welding procedure.

6. The effect of the welding stress relaxation observed in the experiments has the potential to provide a very significant improvement in the interpretation of experimental data for the purpose of residual stress assessment.

7. The period of the welding stress relaxation, observed during the reported experiments, and its final distribution probably depend on both the type and the conditions of the welding, including the geometry (and the dimensions) of the welded specimen. Therefore, it would be interesting to study this relationship to find the minimum time necessary to complete the relaxation of the stresses for each welding technique.

Acknowledgement

References

ALORAIER, A., Al-Mazruoee, A., Price, J.W.H., Shehata, T., (2010) – "Weld repair practices without post weld heat treatment for ferrítica alloys and their consequences on residual stresses: A review". J Press Vessel Pip., 87, pp. 127-133.

ASSIS, J.T., Monin, V., Teodosio, J.R., Gurova, T., (2002) – "X-ray analysis of residual stress distribution in weld region". Adv X-ray Anal., 45, pp. 225-231.

DENG, D., Murakawa, H., (2008) – "Prediction of welding distortion and residual stress in a thin plate butt-welded joint". Comput Mater Sci., 43, pp. 353-365.

GANNON, L., Liu, Y., Pegg, N., Snith, M., (2010) – "Effect of welding sequence on residual stress and distortion in flat-bar stiffened plates". Mar Struct., 23, pp. 385-404.

Gurova, T., Teodosio, J.R., Rebello, J.M., Monin, V., (1997-a) – "Study of the residual stress state during plastic deformation under uniaxial tension in a 5.0Cr and 0.5Mo steel". Scr Mater., 36, pp. 1031-1035.

Gurova, T., Teodosio, J.R., Rebello, J.M., Monin, V., (1997-b) – "Variation of the residual stress state in a welded joint during plastic deformation in a 5.0% Cr and 0.5% Mo steel". J Strain Anal Eng Des., 32, pp. 455-459.

GUROVA, T., Teodosio, J.R., Rebello, J.M., Monin, V., (1998) – "Model for the variation of the residual stress state during plastic deformation under uniaxial tension". J Strain Anal Eng Des., 33, pp. 367-372.

HAUK, V., (1997) – "Structural and residual stress analysis by nondestructive methods, evaluation –application – assessment". Amsterdam: Elsevier Science.

KORSUNSKY, A.M., Regino, G.M., Nowell, D., (2007) – "Variational eigenstrain analysis of residual stresses in a welded plate". J Solids Struct., 44, pp. 4574-4591.

LI, K., Zhang, Y.M., (2007) – "Metal transfer in double-electrode gas metal arc welding". J Manuf Sci Eng., 129, pp. 991-999.

LI, K.H., Zhang, Y.M., (2008) – "Consumable double-electrode GMAW – Part 1: The process". Weld J., 87, pp. 11-17.

LI, K.H., Zhang, Y.M., Xu, P., Yang, F.Q., (2008) – "High-strength steel welding with consumable double-electrode gas metal arc welding". Weld J., 87, Suppl:S57-87.

MACHERAUCH, E., Wohlfahrt, H., (1997) – "Different sources of residual stress as a result of welding". In: Nichols RW (Ed.), Residual stress in welded construction and their effects: An international conference, Nov 15-17, London, Cambridge, Welding Institute, 1978-1979, pp. 267-282.

MONIN, V., Teodosio, J.R., Gurova, T., (2000) – "A portable X-ray apparatus for both stress measurements and phase analysis under field conditions". Adv X-ray Anal., 43, pp. 66-71.

MONIN, V., Teodosio, J.R., Gurova, T., Assis, J., (2000) – "X-ray study of the inhomogeneity of surface residual stresses after shot-peening treatment". Adv X-ray Anal., 43, pp. 48-53.

MONIN, V., Teodosio, J.R., Gurova, T., (2001-a) – "Study and service control of stress state of high-strength steel cables used in prestressed concrete structures". Adv X-ray Anal., 44, pp. 195-200.

MONIN, V., Teodosio, J.R., Gurova, T., (2001-b) – "Analysis of residual stress state in speed gears for automotive vehicles". Adv X-ray Anal., 44, pp. 187-194.

PARADOWSKA, A., Finlayson, T.R., Price, J.W.H., Ibrahim, R., Steuwer, A., Ripley, M., (2006) – "Investigation of the samples for residual strain measurements in a welded specimen by neutron and synchrotron X-ray diffraction". Phy B., 385-386, pp. 904-907.

PARADOWSKA, A.M., Price, J.W.H., Finlayson, T.R., Lienert, U., Walls, P., Ibrahim, R., (2009) – "Residual stress distribution in steel butt welds measured using neutron and synchrotron diffraction". J Phys: Condens Matter 21(12):8.

SCHENK, T., Richardson, I.M., Kraska, M., Ohnimus, S., (2009) – "A study on the influence of clamping on welding distortion". Comput Mater Sci., 45, pp. 999–1005.